Lasers in Manufacturing Conference 2021

Ultrafast pump-probe microscopy reveals the influence of a water layer on the early stage ablation dynamics of gold

Maximilian Spellauge[a,b,*], Carlos Doñate-Buendía[b,c], Stephan Barcikowski[b], Bilal Gökce[b,c], Heinz P. Huber[a]

[a]*Department of Applied Sciences and Mechatronics, Munich University of Applied Sciences, Lothstraße 34, 80335 Munich, Germany*
[b]*Technical Chemistry I and Center for Nanointegration Duisburg-Essen (CENIDE), University of Duisburg-Essen, 45141 Essen, Germany*
[c]*Materials Science and Additive Manufacturing, School of Mechanical Engineering and Safety Engineering, University of Wuppertal, 42119 Wuppertal, Germany*

Abstract

Despite the tremendous amount of research carried out in the field of pulsed laser ablation in liquids, there are only a few works available regarding the early stage ablation dynamics. A description how the liquid influences ablation on time scales ranging from pico- to microseconds would give valuable information regarding the physical processes involved. This work reports on ultrafast pump-probe microscopy measurements of a high purity bulk gold sample immersed in air and water. Our setup enables the observation of transient dynamics ranging from pulse impact on a picosecond timescale to shock wave and cavitation bubble propagation on the nanosecond timescale. We find that the water layer significantly influences the ablation dynamics on the whole investigated temporal range.

Keywords: Laser ablation in liquids; Ultrafast lasers; Pump-probe microscopy; Gold, Nanoparticles

1. Introduction

Laser ablation in liquids (LAL) is a versatile method that enables the generation of surfactant-free and stable nanoparticles with high productivities [1]. The ablation dynamics governing LAL range from plasma generation on a picosecond timescale to cavitation bubble propagation and collapse on a nanosecond to microsecond timescale [2]. Furthermore, compared to laser ablation in gaseous environments, the liquid layer present in

* Corresponding author.
E-mail address: maximilian.spellauge@hm.edu .

LAL adds an additional channel of energy loss [3], represents a highly reactive environment [2], and confines the ablation products [4]. The transient nature of the processes involved during LAL as well as the level of complexity added by the liquid layer makes the experimental investigation of the governing processes challenging. So far, a large body of experimental research focused on LAL ablation dynamics on the nanosecond to microsecond timescale. This includes investigation of plasma generation, confinement of the ablation products by the liquid layer [2], and cavitation bubble propagation [5,6]. However, a complete picture of the dynamical processing occurring on a timescale ranging from sub-nanosecond to microseconds have not been investigated. In order to close this gap in the literature, pump-probe microscopy measurements of the transient reflectivity of a gold target immersed in air and water have been performed.

2. Materials and Methods

Polycrystalline gold (Au) sample with a purity of 99.99% and a thickness of 1 mm were sanded and polished to achieve an average surface roughness of 10 nm. The samples were either immersed in air or in 4 mm of deionized water. A custom build pump-probe microscopy setup was used to investigate the spatial and temporal surface reflectivity dynamics. The pump-pulses which initiated the ablation process had a pulse duration of 3 ps and a wavelength of 1056 nm. Single pump-pulses were focused on the sample surface by a plano-convex lens with a focal length of 100 mm under an incidence angle of $\vartheta = 35°$. This resulted in a beam waist radius of $w_0 = (15 \pm 1)$ µm (at $1/e^2$ intensity level), which was measured under normal incidence by a focal beam profiler (PRIMES GmbH, MicroSpotMonitor). The incident peak fluence Φ_0 on the sample surface was then calculated by the following equation [7]:

$$\Phi_0 = \frac{2 \cdot E_\mathrm{P} \cdot \cos(\vartheta)}{\pi \cdot w_0^2} \tag{1}$$

Here E_P denotes the incident pulse energy. Note that the incidence angle in water decreased to $\vartheta = 25.6°$ due to refraction at the air-water interface. The reflectivity dynamics were recorded using probe-pulses at a pulse duration of 500 fs and wavelength of 528 nm for delay times Δt of up to 4 ns. For Δt exceeding 4 ns, a second electronically triggered laser with a wavelength of 1064 nm and a pulse duration of 600 ps probed the Au surface. A microscope objective (50x, NA = 0.42) was used to focus the probe-pulses onto the sample surface and image the surface onto a CCD camera. For each desired Δt the sample was translated to a pristine surface and a sequence of three images was recorded. The reference image R_0 was taken 5 s before pump-pulse impact and thus represents the reflectivity of the pristine surface. Secondly, the image $R(\Delta t)$ at the desired Δt recorded the transient surface reflectivity after pump-pulse irradiation. Finally, a third image R_inf gives access to the reflectivity 5 s after pump-pulse impact, when the surface is in equilibrium. The transient relative reflectivity change $\Delta R/R_0$ and the final state relative reflectivity change $\Delta R_\mathrm{inf}/R_0$ are then calculated by:

$$\frac{\Delta R}{R_0} = \frac{R(\Delta t) - R_0}{R_0} \tag{2}$$

$$\frac{\Delta R_\mathrm{inf}}{R_0} = \frac{R_\mathrm{inf} - R_0}{R_0} \tag{3}$$

3. Results

The pump-probe microscopy setup described in the materials and methods section has been used to investigate the transient reflectivity dynamics of Au immersed in air and water. Fig. 1 displays the results

after subjecting the Au sample to single pump-pulses with a peak fluence of 3 J/cm^2. The spatially-resolved $\Delta R/R_0$ values are depicted for various Δt, where the left/right half of the images corresponds to irradiation in air/water. The final state $\Delta R_{inf}/R_0$ is indicated at the image labeled "∞".

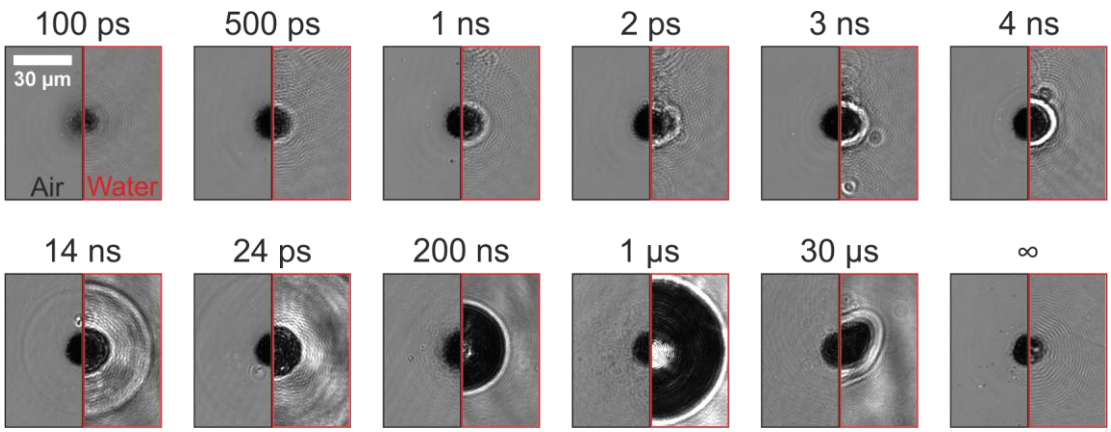

Fig. 1. Transient reflectivity dynamics, recorded after subjecting the Au sample to single pump-pulses with a peak fluence of 3 J/cm^2 in air and water. The left/right half of each image corresponds to irradiation in air/water and the final state relative reflectivity change $\Delta R_{inf}/R_0$ is depicted at the image labeled "∞".

At the first depicted delay time of Δt = 100 ps, a circular region of decreased reflectivity is observed in the central part of the image. With an average $\Delta R/R_0$ value of -0.75 in air and water, the decreased reflectivity and hence increased absorption is approximately independent of the immersion medium. For 500 ps ≤ Δt ≤ 4 ps $\Delta R/R_0$ decreases further to = -0.97 in air, while in water a significantly higher value of -0.9 is observed. When Δt = 14 ns is considered, the reflectivity decrease in water starts to expand radially up to Δt = 1 µs and then shrinks again as depicted at Δt = 30 µs. In the case of air, this expansion is not visible but instead a blurred region of slightly decreased reflectivity surrounding the area of high absorption is visible at Δt = 200 ns. Furthermore, a ring-shaped region of increased reflectivity is visible in water from Δt = 500 ps, while in air this region is first observed at Δt = 3 ns. The ring-shaped region of increased reflectivity propagates outwards with increasing Δt and is no longer visible at Δt = 200 ps. In the final state image, it is observed that the average $\Delta R_{inf}/R_0$ in air (-0.9) is significantly lower compared to water (-0.1).

4. Discussion

The similar decreased reflectivity and hence increased absorption observed at Δt = 100 ps hints towards photo-thermal phase explosion as the ablation mechanism in air and water, since the photo-thermally produced gas-liquid mixture results in scattering and absorption of the incident probe-pulse [8–10]. Starting from Δt = 500 ps, the absorption in water is less pronounced compared to air. This behavior is attributed to the confinement of the ablation products by the water layer [4,11]. In air the ablation products propagate freely into the surrounding atmosphere and since a sharp boundary at the air-plume interface is not present, almost all the incoming probe-pulse radiation is scattered and absorbed in the ablation plume. However, in water the confinement of the ablation plume by the water layer leads to the formation of an air-water boundary. Fresnel-like reflection at this boundary results in the observed increased reflectivity compared to air. The ring-shaped region of increased reflectivity has previously been attributed to an outwards propagating

pressure wave, while the area of outwards propagating decreased reflectivity in water is attributed to the cavitation bubble [6]. From this observation it is concluded that pressure wave and cavitation bubble formation in water already occur at a delay time of Δt = 500 ps. Furthermore, separation of the pressure wave from the cavitation bubble occurs on a later timescale and is first observed at Δt = 14 ns. Finally, the higher final state absorption in air compared to water is ascribed to the higher surface roughness obtained after ablation in air [12]. The higher surface roughness in air leads to increased scattering [13] and thus to a decreased reflectivity compared water.

5. Conclusion

Laser ablation in liquids is a versatile and flexible method to fabricate nanoparticles. Despite the tremendous amount of research in the field, experimental investigation of the ablation dynamics on a sub-nanosecond timescale is still lacking. In order to fill this gap, time- and space-resolved reflectivity measurements have been performed by utilizing a pump-probe microscopy setup. It was found that the water layer significantly influences the reflectivity dynamics on the entire investigated timescale. The results presented here advance the understanding of the ablation process in liquids and are thus promising for further optimization of the process regrading efficiency and control of particle size.

Acknowledgements

The authors gratefully acknowledge financial support of this work by the Deutsche Forschungsgemeinschaft (DFG) grants HU 1893/6-1, GO 2566/7-1, GO 2566/8-1 and GO 2566/10-1. B. Gökce additionally acknowledges funding from the DFG within the Heisenberg Program, project GO 2566/10-1.

References

[1] D. Zhang, B. Gökce, S. Barcikowski, Laser Synthesis and Processing of Colloids: Fundamentals and Applications, Chem. Rev. 117 (2017) 3990–4103. https://doi.org/10.1021/acs.chemrev.6b00468.

[2] A. Kanitz, M.-R. Kalus, E.L. Gurevich, A. Ostendorf, S. Barcikowski, D. Amans, Review on experimental and theoretical investigations of the early stage, femtoseconds to microseconds processes during laser ablation in liquid-phase for the synthesis of colloidal nanoparticles, Plasma Sources Sci. Technol. 28 (2019) 103001. https://doi.org/10.1088/1361-6595/ab3dbe.

[3] S. Dittrich, S. Barcikowski, B. Gökce, Plasma and nanoparticle shielding during pulsed laser ablation in liquids cause ablation efficiency decrease, Opto-Electronic Adv. 4 (2021) 20007201–20007215. https://doi.org/10.29026/oea.2021.200072.

[4] A. Kanitz, D.J. Förster, J.S. Hoppius, R. Weber, A. Ostendorf, E.L. Gurevich, Pump-probe microscopy of femtosecond laser ablation in air and liquids, Appl. Surf. Sci. 475 (2019) 204–210. https://doi.org/10.1016/j.apsusc.2018.12.184.

[5] J. Tomko, S.M. O'Malley, C. Trout, J.J. Naddeo, R. Jimenez, J.C. Griepenburg, W. Soliman, D.M. Bubb, Cavitation bubble dynamics and nanoparticle size distributions in laser ablation in liquids, Colloids Surfaces A Physicochem. Eng. Asp. 522 (2017) 368–372. https://doi.org/10.1016/j.colsurfa.2017.03.030.

[6] J. Long, M. Eliceiri, Z. Vangelatos, Y. Rho, L. Wang, Z. Su, X. Xie, Y. Zhang, C.P. Grigoropoulos, Early dynamics of cavitation bubbles generated during ns laser ablation of submerged targets, Opt. Express. 28 (2020) 14300. https://doi.org/10.1364/OE.391584.

[7] P. Boerner, M. Hajri, T. Wahl, J. Weixler, K. Wegener, Picosecond pulsed laser ablation of dielectric rods: Angle-dependent ablation process model for laser micromachining, J. Appl. Phys. 125 (2019) 234902. https://doi.org/10.1063/1.5092812.

[8] C. Pan, L. Jiang, J. Sun, Q. Wang, F. Wang, K. Wang, Y. Lu, Y. Wang, L. Qu, T. Cui, Ultrafast optical response and ablation

mechanisms of molybdenum disulfide under intense femtosecond laser irradiation, Light Sci. Appl. 9 (2020) 80. https://doi.org/10.1038/s41377-020-0318-8.

[9] M. Spellauge, J. Winter, S. Rapp, C. McDonnell, F. Sotier, M. Schmidt, H.P. Huber, Influence of stress confinement, particle shielding and re-deposition on the ultrashort pulse laser ablation of metals revealed by ultrafast time-resolved experiments, Appl. Surf. Sci. 545 (2021) 148930. https://doi.org/10.1016/j.apsusc.2021.148930.

[10] J. Winter, S. Rapp, M. Spellauge, C. Eulenkamp, M. Schmidt, H.P. Huber, Ultrafast pump-probe ellipsometry and microscopy reveal the surface dynamics of femtosecond laser ablation of aluminium and stainless steel, Appl. Surf. Sci. 511 (2020) 145514. https://doi.org/10.1016/j.apsusc.2020.145514.

[11] C.-Y. Shih, M. V. Shugaev, C. Wu, L. V. Zhigilei, Generation of Subsurface Voids, Incubation Effect, and Formation of Nanoparticles in Short Pulse Laser Interactions with Bulk Metal Targets in Liquid: Molecular Dynamics Study, J. Phys. Chem. C. 121 (2017) 16549–16567. https://doi.org/10.1021/acs.jpcc.7b02301.

[12] C.-Y. Shih, I. Gnilitskyi, M. V. Shugaev, E. Skoulas, E. Stratakis, L. V. Zhigilei, Effect of a liquid environment on single-pulse generation of laser induced periodic surface structures and nanoparticles, Nanoscale. (2020). https://doi.org/10.1039/D0NR00269K.

[13] D. Bergström, J. Powell, A.F.H. Kaplan, The absorption of light by rough metal surfaces—A three-dimensional ray-tracing analysis, J. Appl. Phys. 103 (2008) 103515. https://doi.org/10.1063/1.2930808.